Luminescence enhancement and quenching by codopant ions in lanthanide doped fluoride nanocrystals

2011 Nanotechnology 22 175702

(http://iopscience.iop.org/0957-4484/22/17/175702)

Nanotechnology **22** (2011) 175702 (5pp) doi:10.1088/0957-4484/22/17/175702

Luminescence enhancement and quenching by codopant ions in lanthanide doped fluoride nanocrystals

Dangli Gao[1], Hairong Zheng[1,3], Xiangyu Zhang[2], Wei Gao[1], Yu Tian[1], Jiao Li[1] and Min Cui[1]

[1] College of Physics and Information Technology, Shaanxi Normal University, Xi'an 710062, Shaanxi, People's Republic of China
[2] College of Physics and Electronic Information Engineering, Qinghai Nationalities University, Xining 810007, Qinghai, People's Republic of China

E-mail: hrzheng@snnu.edu.cn

Received 7 January 2011, in final form 20 February 2011
Published 16 March 2011
Online at stacks.iop.org/Nano/22/175702

Abstract
Luminescence enhancement (LE) and quenching for lanthanide (Ln) doped nanocrystals is obtained by a second Ln^{3+} ion doping method. Singly or doubly doped LaOF, LaF_3 and $NaYF_4$ nanocrystals are studied in detail under selective or two-color excitations. The underlying reason for LE by codoping is explored, and a mechanism of the enhancement based on the low local point symmetry effect of the matrix is proposed. It is found that the modification of the local environment induced by dopant ions can result in LE if the non-radiative relaxation probability can be ignored. The observations reported here should be useful for improving the quality of Ln^{3+} doped nanomaterials.

(Some figures in this article are in colour only in the electronic version)

1. Introduction

Lanthanide (Ln) doped nanomaterials (NMs) show superior chemical and optical properties, including low toxicity, large effective Stokes shifts, sharp emission bands, weak background luminescence as well as high resistance to photobleaching, blinking, and photochemical degradation [1–4]. These unique properties, coupled with size- and shape-independent luminescent phenomena, make Ln^{3+} doped nanocrystals (NCs) have applications in a very wide range of fields. Lasers, infrared quantum counters, new-generation lighting, three-dimensional displays and biological probes are good examples of their applications [5–7]. Unfortunately, these Ln^{3+} doped NMs usually have low emission efficiency because of their structure defects and large surface area with a variety of quenchers. Furthermore, the small absorption cross-section to the excitation light also limits the luminescence efficiency. Therefore, how to enhance the emission is one of the most important issues for developing the application of Ln^{3+} doped NMs. Many strategies have been used to enhance the luminescence, which include the adjustment of shape, size, crystal phase of NCs and the dopant concentration [2]. Introducing hybridization, surface modification [4], and metal substrates to enhance the luminescence [5] have also been used for this purpose. But most of these are either hard to implement or only suitable for individual Ln^{3+} ions.

Codoping is a widely applied technological process in Ln^{3+} doped luminescent materials science that involves incorporating atoms or ions of appropriate elements into host lattices, to yield hybrid materials with desirable properties such as modifying the electronic properties [8], stabilizing a specific crystallographic phase [9] or tuning emission properties [10]. It has been reported that doping other ions such as Li^+, Al^{3+} and Zn^{2+} can also significantly enhance the luminescence in $GdTaO_4$:Eu^{3+} [11]. The enhancement effect of various doped ions could even be associated with the effective ionic radius of the codopant ions and the mismatch of electronegativity between the doping ions and Gd^{3+}. However, the explicit reason for the enhancement of luminescence by doping ions is not yet very clear.

In this study, we attempted to obtain an enhanced luminescence effect in Ln^{3+} doped LaF_3, LaOF and $NaYF_4$

[3] Author to whom any correspondence should be addressed.

NCs by codoping a second Ln^{3+} ion. Three kinds of matrix systems with singly or doubly doped Ln^{3+} ions have been studied in detail under selective excitation or two-color excitation. Investigations on the emission spectrum, luminescence lifetime and quantum efficiency have been carried out, and a mechanism of the luminescence enhancement (LE) and quenching (LQ) is revealed.

2. Experimental details

Ln^{3+} doped LaF_3, LaOF and $NaYF_4$ NCs were synthesized by employing the methods presented in [12, 13]. The composition of the samples used in this study was in mol%. In a typical procedure for the synthesis of Ln doped LaF_3 NCs, 1.2 ml of 0.5 mol l^{-1} $Ln(NO_3)_3$ (Ln = La, Yb, Gd, Tb and Pr) were selectively added to 30 ml of deionized water under stirring, followed by the addition of 2.4 ml of sodium fluoride solution (NaF, 1.0 mol l^{-1}) and thorough stirring. Then the colloidal solution was transferred into a 40 ml Teflon-lined autoclave and heated at 200 °C for 16 h. The final product (LaF_3) was collected by centrifuging, and washed with water and ethanol. The collected LaF_3 NCs were dried at 60 °C for 12 h. Ln^{3+} doped LaOF NCs were produced by thermally treating LaF_3:Ln^{3+} NCs at 800 °C for several hours.

For the synthesis of $NaYF_4$:Ln^{3+} nanorods, 0.6 mmol of rare-earth (RE) nitrate (1.2 ml of 0.5 mol l^{-1} $RE(NO_3)_3$, RE = Y, Eu, Tm, Ce, Gd, Tb, Sm and Pr) aqueous solution and sodium fluoride solution(4.0 ml, 1.0 mol l^{-1}) were added to a mixture of NaOH (0.6 g), ethanol (10.0 ml), deionized water (3.0 ml), and oleic acid (10.0 ml). The solution was then thoroughly stirred. Subsequently, the milky colloidal solution was transferred to a 40 ml Teflon-lined autoclave, and heated at 190 °C for 20 h. The final product ($NaYF_4$) was collected by centrifuging, and washed with water and ethanol. The collected NCs were dried under 60 °C for 12 h.

The phase compositions of the as-prepared products were examined by x-ray diffraction (XRD) with a D/Max2550VB+/PC x-ray diffraction meter with Cu Kα (40 kV, 40 mA) irradiation (λ = 0.154 06 nm). The typical XRD patterns of LaF_3, LaOF and $NaYF_4$ are shown in the lower part of figure 1. All of the strong and sharp reflection peaks in (a)–(c) can be readily indexed as the pure hexagonal phase of LaF_3, tetragonal phase of LaOF and hexagonal phase of $NaYF_4$, respectively. No other impurity phases were observed. Further morphological analysis of the samples was performed by TEM, using a JEM 2100 transmission electron microscope operating at an acceleration voltage of 200 kV. The upper part of figure 1 shows the typical TEM images of the three samples. LaF_3 and LaOF NCs of about 30 nm size were observed in (a) and (b). It is noted that the LaOF NCs present a relatively greater degree of agglomeration than LaF_3. High quality monodisperse and uniform sizes of $NaYF_4$ NCs with diameters of about 35 nm can be observed in (c).

During the spectroscopic measurements, YAG:Nd^{3+} (Quanta Ray Lab-170) and He–Cd (MMF-12B24DH-F00) continuum lasers were employed as excitation sources. The resonant excitation was performed by a pulsed dye laser (Sirah) equipped with a second harmonic generation

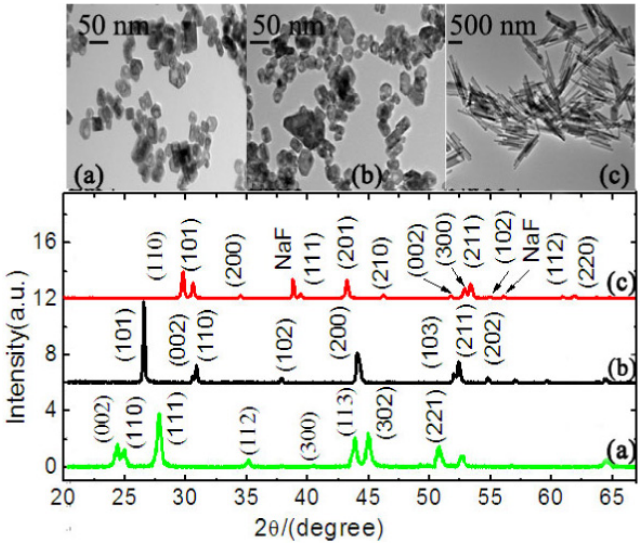

Figure 1. XRD patterns and TEM images of 1.0% Eu^{3+} doped LaF_3 (a), LaOF (b) and $NaYF_4$ (c) NCs.

crystal. A monochromator (SP 2750i) with a spectral resolution of approximately 0.008 nm and a charge coupled device (ACTON, PIXIS 100) were used for luminescence collection and detection. For the time domain luminescence measurements, a TDS 5000 B digital storage oscilloscope (Tektronix) was employed. The corresponding notch filters were placed in front of the entrance of the monochromator to block the scattered light. All measurements were carried out at room temperature.

3. Results and discussion

Part of the f-electronic levels for Eu^{3+} ions along with main transitions are indicated in figure 2(d), and the luminescence spectra of LaOF:Tm^{3+}/Eu^{3+}, LaOF:Eu^{3+} and LaOF:Tm^{3+} NCs are shown in figures 2(a)–(c). When the Tm^{3+} ions are selectively excited to the $^1D_2$ electronic level with 354.5 nm photons, significant enhancements on the blue emission from Tm^{3+} and red emission from Eu^{3+} were observed in codoped NCs relative to their singly doped counterparts (figure 2(a)). The enhancement factors of blue and red emissions are 2.4 and 10.0, respectively. Pumping Eu^{3+} to $^5D_4$ level with 349.0 nm photons, the same order of magnitude LE was observed in LaOF:Tm^{3+}/Eu^{3+} NCs (figure 2(b)). Enhanced luminescence from Eu^{3+} was also obtained when the Eu^{3+} ions are selectively excited with 532.0 nm photons (figure 2(c)), which indicated that LE is independent of the excitation wavelength and luminescent energy level.

We consider that other measurements, where Eu^{3+} and Pr^{3+} ions were excited simultaneously with a two-color experiment, are necessary for an adequate interpretation of the LE and LQ effects in LaOF NCs. As is shown in figure 3, the luminescence intensity decreases and spectral lines become narrower in Pr^{3+} codoped LaOF:Eu^{3+} NCs (figure 3(b)) relative to their singly doped counterparts (figures 3(a) and (c)). For example, the full width at half maximum values of the

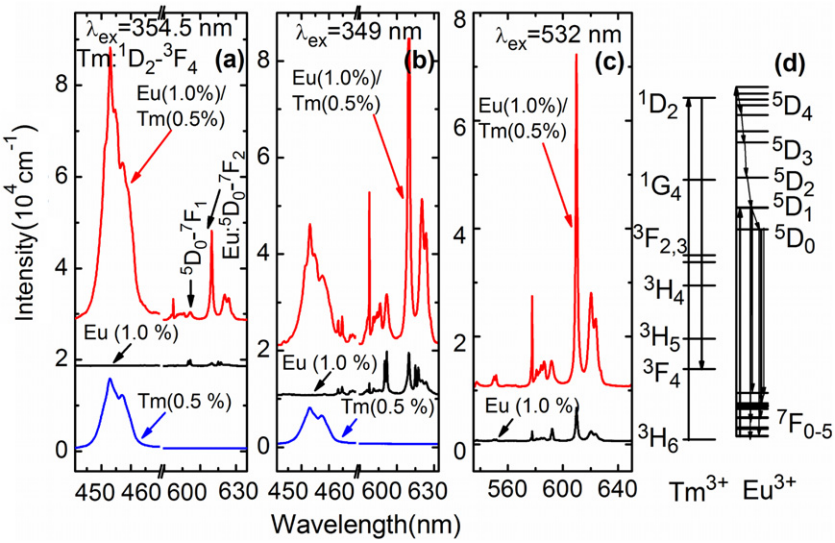

Figure 2. Emission spectra of Ln^{3+} doped LaOF NCs ((a)–(c)) and energy level diagram of Ln^{3+} (d). The corresponding excitation wavelength and doping ions have been marked in the figure.

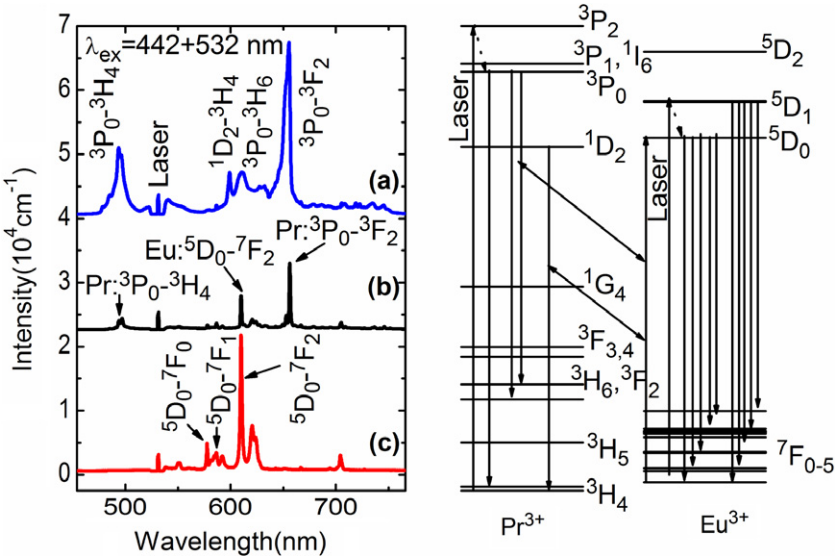

Figure 3. Emission spectra of LaOF NCs under two-color excitation (left) and energy level diagram of Ln^{3+} (right). (a) LaOF:Pr^{3+}(1.0%); (b) LaOF:Eu^{3+}(1.0%)/Pr^{3+}(1.0%); (c) LaOF:Eu^{3+}(1.0%).

linewidth at 610 nm for Eu^{3+} is 1.40 nm in LaOF:Eu^{3+}/Pr^{3+} NCs, while it is 1.94 nm in LaOF:Eu^{3+} NCs.

The reasons for LE and LQ induced by codoping a second Ln^{3+} could be complex. The substitution of the Ln^{3+} into the host lattice and any tendency of the Ln^{3+} to cluster will invalidate interpretations based on a random distribution [14]. But the complications in the current study could stem from two sources: one is that some additional non-radiative decay channels are introduced by a second doping Ln^{3+}, the other is that the doping process may generate changes in the site symmetry of the crystal field acting on the ion.

Figure 2 shows that the ratio of the luminescence intensity of $^5D_0$–$^7F_1$ to $^5D_0$–$^7F_2$ transitions from LaOF:Eu^{3+}/Tm^{3+} NCs is smaller than that from LaOF:Eu^{3+} NCs, leading us to conclude that the variation of the site symmetry of the crystal field are more significant in LaOF:Tm^{3+}/Eu^{3+} NCs compared with LaOF:Eu^{3+} NCs [15].

The modification of the linewidth and structure of the luminescence spectra in (La, Eu, Pr) OF crystals indicate that many factors might be responsible for the LQ induced by Pr^{3+}. The ionic radius of 101.3 pm for Pr^{3+} is very close to that of 106.1 pm for La^{3+}, as compared with 86.9 pm for Tm^{3+} [16]. It is reasonable that the lattice distortion is smaller in LaOF:Pr^{3+}/Eu^{3+} than that in LaOF:Tm^{3+}/Eu^{3+} NCs [15]. However, this cannot explain the experimental observations that the luminescence intensity is weaker and the linewidth smaller in LaOF:Pr^{3+}/Eu^{3+} NCs than that in LaOF:Pr^{3+} NCs (figures 3(a) and (b)).

The f–f transitions of Ln^{3+} are parity forbidden transitions [4] and the non-radiative energy transfer effect

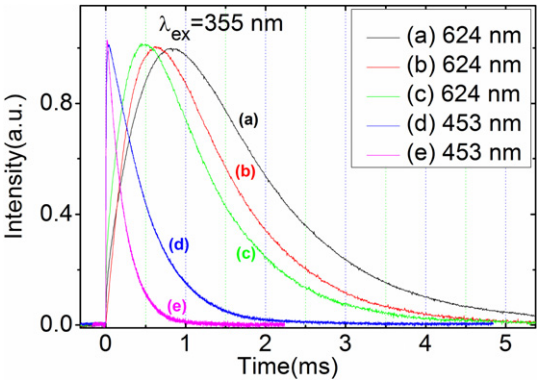

Figure 4. Decay profiles of the luminescence at 624 nm of Eu^{3+} and 453 nm of Tm^{3+} in LaOF NCs after 355.0 nm photon excitation. (a) LaOF:Eu^{3+}(1.0%); (b) LaOF:Tm^{3+}(1.0%)/Eu^{3+}(1.0%); (c) LaOF:Pr^{3+}(1.0%)/Eu^{3+}(1.0%); (d) LaOF:Tm^{3+}(1.0%); (e) LaOF:Tm^{3+}(1.0%)/Eu^{3+}(1.0%). The corresponding monitored wavelengths have been marked in the chart.

Table 1. The lifetime, RTP and IQE of $^5D_0(Eu^{3+})$ level in different samples, n is refractive index of the matrix.

Sample	LaOF:Eu^{3+}	LaOF:Eu^{3+}/Tm^{3+}	LaOF:Eu^{3+}/Pr^{3+}
τ_{obs} (μs)	1280	920	880
K_{rad} (s^{-1})	$133n^3$	$297n^3$	$168n^3$
η%	$17.0n^3$	$27.0n^3$	$14.7n^3$

tends to be more pronounced in a system with forbidden transitions [17]. As shown in figure 2, it is possible that cross-relaxations induced by Pr^{3+} quench the luminescence of some energy levels and subsequently narrow the luminescence linewidth in LaOF:Eu^{3+}/Pr^{3+} NCs due to matching of energy levels between Pr^{3+} and Eu^{3+}.

Time-dependent luminescence measurements provide an attractive way of detecting the local environment of dopant ions. The luminescence decays of $^1D_2(Tm^{3+})$ and $^5D_0(Eu^{3+})$ levels are shown in figure 4. It was found that the decay of the $^1D_2(Tm^{3+})$ level is mainly single exponential (figures 4(d) and (e)). The decay times are found to be 482 μs for LaOF:Tm^{3+} NCs and 330 μs for LaOF:Tm^{3+}/Eu^{3+} NCs. The luminescence decay for the $^5D_0(Eu^{3+})$ level is presented as a non-exponential (figures 4(a)–(c)). The rise time for the decay curve stands for the non-radiative relaxation time from $^5D_1$level to $^5D_0$ level, while the decline time stands for the luminescence lifetime of $^5D_0$ level. The long components obtained from the data fitting to the decay curves are listed in table 1, which are contributed by the ions away from the surface defects [18]. One can see that the luminescence lifetime decreases in codoped samples (figures 4(b), (c) and (e)) compared with their singly doped counterparts (figures 4(a), (d) and table 1).

The intensity decay of luminescence emission is determined by the radiative transition probability (RTP) K_{rad} and the non-radiative relaxation probability (NRRP) K_{non} that is due to the interaction of the fluorescing ion with its surroundings. The experimentally measured quantities are the luminescence lifetime and the intrinsic quantum efficiency (IQE), which are defined as follows [19]

$$\tau_{obs} = 1/(K_{rad} + K_{non}) \quad (1)$$

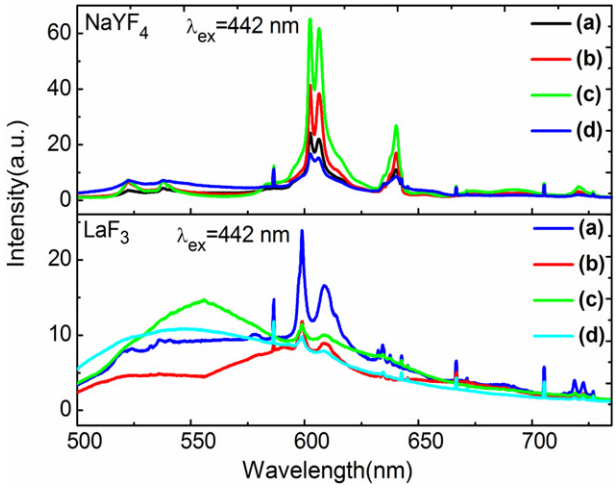

Figure 5. Emission spectra of LaF_3 NCs and $NaYF_4$ NCs doped with Ln^{3+}. The corresponding dopant concentrations are (a) Pr^{3+}(5.0%); (b) Pr^{3+}(5.0%)/Eu^{3+}(1.0%); (c) Pr^{3+}(5.0%)/Tb^{3+}(1.0%) and (d) Pr^{3+}(5.0%)/Ho^{3+}(1.0%).

$$\eta = K_{rad}/(K_{rad} + K_{non}) = K_{rad}/K_{obs} = \tau_{obs}/\tau_{rad} \quad (2)$$

where η is the IQE that reflects the extent of non-radiative deactivation processes of the ion. The observed rate constant K_{obs} is the sum of the rates of the various deactivation processes. $\tau_{obs} = 1/K_{obs}$ represents the lifetime of the excited state.

The europium ion has an isolated magnetic dipole transition ($^5D_0 \rightarrow ^7F_1$), therefore the RTP of its $^5D_0$ level can be written as [20]

$$K_{rad} = A_{MD,0}n^3(I_{tot}/I_{MD}) \quad (3)$$

where $A_{MD,0}$ is the magnetic dipole transition constant, which equals 14.65 s^{-1}. n is the refractive index of the matrix and I_{tot}/I_{MD} is the ratio of the total integrated $^5D_0 \rightarrow ^7F_j$ ($j = 0$–6) emission to that of the $^5D_0 \rightarrow ^7F_1$ transition. Based on equations (2) and (3), the τ_{rad} of $^5D_0(Eu^{3+})$ and the IQE from different samples are obtained and listed in the table 1.

If the variation was purely due to the change in K_{non}, then both η and τ would vary in the same manner. Table 1 shows that in general this is not the case. The results of IQE and the lifetime of $^5D_0$ (Eu^{3+}) from the three samples indicate that the increase of RTP is mainly responsible for the increase of luminescence intensity in LaOF:Tm^{3+}/Eu^{3+} NCs, while the NRRP introduced by a dopant is mainly responsible for the LQ in LaOF:Pr^{3+}/Eu^{3+} NCs.

To verify the mechanism of LE and LQ by Ln^{3+} dopant control, several kinds of Ln^{3+} ions were doped into different host lattices. Figure 5 shows the emission spectra of two set samples including LaF_3:Pr^{3+}(1.0%)/Ln^{3+} (0% or 1.0%) (Ln = Eu, Tb and Ho) and $NaYF_4$:Pr^{3+}(1.0%)/Ln^{3+} (0% or 1.0%) (Ln = Eu, Tb and Ho) NCs. The LE was obtained in $NaYF_4$:Pr^{3+}/Eu^{3+}(Tb^{3+}) NCs that have low phonon energy [21] except for $NaYF_4$:Pr^{3+}/Ho^{3+} NCs due to meeting the energy-matching requirements. The luminescence for another series of LaF_3NCs doped with Ln^{3+} was quenched by codoping ions. It seems that the LE effect depends on

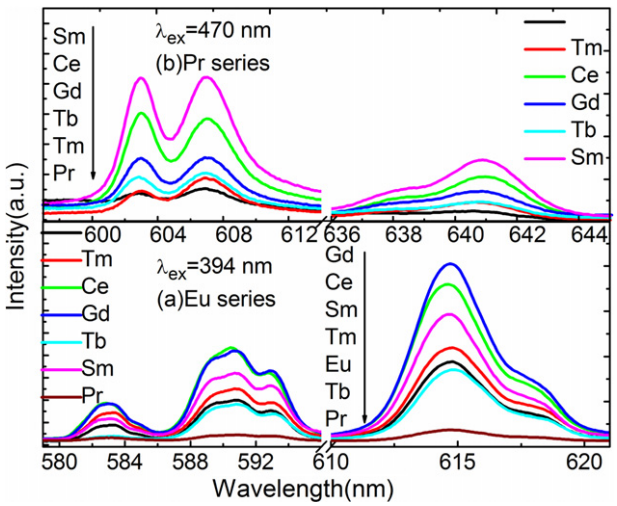

Figure 6. Emission spectra of $NaYF_4$:Eu^{3+} NCs and $NaYF_4$:Pr^{3+} NCs codoped with the second Ln^{3+}. (a) is the Eu^{3+} doped series and (b) is the Pr^{3+} doped series. The second dopant Ln^{3+} ions have been marked in the figure.

the energy of host lattice phonons and the energy mismatch between luminescence ions and doping ions. For example, when a second codopant Ln^{3+}, which has simple energy level configuration such as Sm^{3+}, Gd^{3+} or Ce^{3+}, was doped into $NaYF_4$ host lattice, LE was observed (figure 6). No dopant ionic-radius dependence is found in the LE and LQ effect. It is well known that the electric-dipole (ED) transition of Ln^{3+} is forbidden by parity selection. However, such a transition was relaxed by a low symmetry host lattice [22]. Chen *et al* [23] found that the strong luminescence originates from Eu^{3+} occupying a low symmetry site of C_2, but not a centrosymmetric site of S_6 in cubic Gd_2O_3. Morrison *et al* [24, 25] summarized the crystal-field spectra of Ln^{3+} for 26 types of host crystals with different symmetries. Similarly, dopant ions introduced into the centrosymmetric site of the lattice may produce lattice distortion and low symmetry sites [26], which make luminescent ions experience a drastic change of local crystal-field environment [27]. Therefore, we could conclude that the LE effect originates from the induced change by doping ions in the site symmetry of the crystal field acting on the luminescence ions, while the LQ effect originates from additional non-radiative decay channels induced by a second doping. Whether the luminescence was enhanced or not depends on the ratio of RTP to NRRP of luminescent level.

4. Conclusion

In summary, the LE and LQ effect has been investigated systematically when a second Ln^{3+} ion was codoped into nanoscale materials. The influence of the matrix phonon energy, the energy level structure of luminescence ions, the energy mismatch between Ln^{3+} ions, and the ionic radius of the second Ln^{3+} on the luminescence intensity of Eu^{3+} have been investigated in detail. The results suggest that the second dopant Ln^{3+} in NCs can introduce an additional non-radiative decay channel to the luminescence level and modify the local environment of luminescence Ln^{3+} ions, which results in a more rapid decay of the luminescence signal and the modified luminescence intensity. Whether the luminescence was enhanced or quenched depends on the ratio of RTP to NRRP of the luminescent level. The modification of the local environment induced by dopant ions results in LE when the non-radiative relaxation probability is ignored. The reported LE and LQ effect should be useful for testing the non-radiative decay channel of Ln^{3+} doped NMs and could provide general criteria for examining the optical quality of Ln^{3+} doped NMs.

Acknowledgments

This work is supported by the Fundamental Research Funds for the Central Universities (Grant No. GK200901022) and the Innovation Funds of Graduate Programs (Grant No. 2009 CXB005), SNNU.

References

[1] Wang F, Tan W B, Zhang Y, Fan X P and Wang M Q 2006 *Nanotechnology* **17** R1–13
[2] Li P, Peng Q and Li Y D 2009 *Adv. Mater.* **21** 1945–8
[3] Mahalingam V, Vetrone F, Naccache R, Speghini A and Capobianco J A 2009 *Adv. Mater.* **21** 4025–8
[4] Eliseeva S V and Bunzli J-C G 2010 *Chem. Soc. Rev.* **39** 189–227
[5] Feng W, Sun L-D and Yan C-H 2009 *Chem. Commun.* **5** 4393–5
[6] Di W, Li J, Shirahata N and Sakka Y 2010 *Nanotechnology* **21** 455703
[7] Yu X F, Li M, Xie M Y, Chen L D, Li Y and Wang Q Q 2010 *Nano Res.* **3** 51–60
[8] Alivisatos A P 1996 *Science* **271** 933–7
[9] Wang F, Han Y, Lim C S, Lu Y H, Wang J, Xu J, Chen H Y, Zhang C, Hong M H and Liu X G 2010 *Nature* **463** 1061–5
[10] Wang F and Liu X G 2008 *J. Am. Chem. Soc.* **130** 5642–3
[11] Liu B, Gu M, Liu X L, Han K, Huang S M, Ni C, Zhang G B and Qi Z M 2009 *Appl. Phys. Lett.* **94** 061906
[12] Wang X, Zhuang J, Peng Q and Li Y D 2005 *Nature* **437** 121–4
[13] He E J, Zheng H R, Zhang Z L, Zhang X S, Xu L M, Fu Z X and Lei Y 2010 *J. Nanosci. Nanotechnol.* **10** 1908–12
[14] Brown M R, Whiting J S S and Shand W A 1965 *J. Chem. Phys.* **43** 1–9
[15] Stouwdam J W and van Veggel F C J M 2002 *Nano Lett.* **2** 733–7
[16] Templeton D H and Dauben C H 1954 *J. Am. Chem. Soc.* **76** 5237–9
[17] Auzel F 2004 *Chem. Rev.* **104** 139–73
[18] Zheng H R, Gao D L, Zhang X Y, He E J and Zhang X S 2008 *J. Appl. Phys.* **104** 013506
[19] Kaminskii A A 1996 *Crystalline Lasers: Physical Process and Operating Schemes* (Boca Raton, FL: CRC Press)
[20] Werts M H V, Jukes R T F and Verhoeven J W 2002 *Phys. Chem. Chem. Phys.* **4** 1542–8
[21] Menyuk N, Dwight K and Pinaud F 1972 *Appl. Phys. Lett.* **21** 159–61
[22] Judd B R 1962 *Phys. Rev.* **127** 750–61
[23] Liu L Q and Chen X Y 2007 *Nanotechnology* **18** 255704
[24] Chen X Y and Liu G K 2005 *J. Solid State Chem.* **178** 419–28
[25] Morrison C A and Leavitt R P 1982 *Handbook on the Physics and Chemistry of Rare Earths* vol 5, ed K A Gschneidner Jr and L Eyring (Amsterdam: North-Holland)
[26] Gao D L, Zheng H R, Zhang X Y, Fu Z X, Zhang Z L, Tian Y and Cui M 2011 *Appl. Phys. Lett.* **98** 011907
[27] Liu L Q, Ma E, Li R F, Liu G K and Chen X Y 2007 *Nanotechnology* **18** 015403